

Spatial field correlation, the building block of mesoscopic fluctuations

P. Sebbah,¹ B. Hu,² A. Z. Genack,² R. Pnini,³ and B. Shapiro³

¹*Laboratoire de Physique de la Matière Condensée,*

Université de Nice - Sophia Antipolis,

Parc Valrose, 06108, Nice Cedex 02, France

²*Department of Physics, Queens College of the City*

University of New York, Flushing, New York 11367

³*Department of Physics, Technion-Israel Institute of Technology, Haifa 32000, Israel*

(Dated: February 1, 2008)

Abstract

The absence of self averaging in mesoscopic systems is a consequence of long-range intensity correlation. Microwave measurements suggest and diagrammatic calculations confirm that the correlation function of the normalized intensity with displacement of the source and detector, ΔR and Δr , respectively, can be expressed as the sum of three terms, with distinctive spatial dependences. Each term involves only the sum or the product of the square of the field correlation function, $F \equiv F_E^2$. The leading-order term is the product, the next term is proportional to the sum. The third term is proportional to $[F(\Delta R)F(\Delta r) + [F(\Delta R) + F(\Delta r)] + 1]$.

PACS numbers: 41.20.Jb, 05.40.-a, 71.55.Jv

Short-range correlation in waves transmitted through random media is manifest in the intensity speckle pattern. The leading contribution, C_1 , to the cumulant correlation function C of intensity normalized to its ensemble average on the output surface of the sample is given by the square of the field correlation function, $C_1 = F_E^2$. Neglecting internal reflection from the surface, its dependence upon displacement Δr on the output surface is given by $C_1(\Delta r) = F_E^2(\Delta r) \equiv F(\Delta r) = (\sin k\Delta r/k\Delta r)^2 \exp(-\Delta r/\ell_s)$, where k is the wave vector and ℓ_s is the scattering mean free path [1]. This term dominates intensity fluctuations. Defining a correlation length, δr , as the first zero of C_1 gives $\delta r = \pi/k = \lambda/2$. The intensity is correlated far beyond δr as a result of scattering within the medium [2, 3, 4, 5, 6, 7] so that intensity values in remote speckle spots are not statistically independent. This gives rise to two additional contributions to C , which can therefore be expressed as, $C = C_1 + C_2 + C_3$ [3, 8], and leads to greatly enhanced mesoscopic fluctuations [9]. The C_2 term produces an enhancement in total transmission fluctuations over that given by the field factorization approximation by a factor of L/ℓ , where ℓ is the transport mean free path and L is the sample length [2, 7]. The C_3 term is the source of universal conductance fluctuations, which are enhanced by a factor of $(L/\ell)^2$ [9, 10]. The magnitude of C_1 at a point is unity as a result of normalization, whereas the magnitudes of C_2 and C_3 are expansions in $1/g$ with leading terms of order $1/g$ and $1/g^2$ [3], respectively, where g is the dimensionless conductance. Since the onset of localization is at $g = 1$ [11], the two terms beyond the field factorization approximation for C , reflect the approach to localization.

In this Letter, we use microwave measurements and diagrammatic calculations to show that each of the contributions to C may be expressed in terms of the square of the field correlation function with regard to displacements of the source, ΔR and detector, Δr . The C_1 term is $F(\Delta R)F(\Delta r)$, the C_2 term is proportional to $[F(\Delta R) + F(\Delta r)]$, while the C_3 term is proportional to $[F(\Delta R)F(\Delta r) + [F(\Delta R) + F(\Delta r)] + 1]$. When the intensity correlation is considered at a shifted frequency, $\Delta\nu$, the full correlation function remains a sum of three terms each being a product of the corresponding terms in C , thus, $C_i = A_i(\Delta\nu)C_i(\Delta r, \Delta R)$ ($i = 1, 2, 3$). Absorption alters the magnitudes of C_2 and C_3 , but it does not change the spatial structure of these terms.

Initial measurements of angular intensity correlation, carried out in the far field of weakly scattering media, gave C , which was essentially equal to C_1 [12, 13]. Recently, measurements of the spatial correlation of the field on the sample surface have yielded the C_1 contribution

directly [14]. Measurements of intensity correlation between points on the sample surface and the interior of the sample on a scale greater than the wavelength have allowed the observation of C_2 [5]. In addition measurements have been made of the spectral correlation of the C_1 [15] and C_2 terms [16, 17, 18] and of the temporal correlation of the C_1 [19], C_2 [20] and C_3 [21] terms in colloidal samples. However, the variation of C on a subwavelength scale, as well as the structure of correlation with displacement of both the source and detector, have not been reported previously. The present measurements and calculations allow us to discern the structure of intensity correlation and to relate it to the correlation of the underlying field.

Measurements are made in a disordered dielectric sample contained within a reflecting tube. Radiation of frequency ν emitted by a source antenna at \vec{R} at one end of the tube is detected at a point \vec{r} at the other end. We denote the intensity at \vec{r} due to a source at \vec{R} by $I_\nu(\vec{r}, \vec{R})$ and consider the normalized cumulant correlation function,

$$C(\Delta r, \Delta R) \equiv \langle \delta I_\nu(\vec{r}, \vec{R}) \delta I_{\nu'}(\vec{r}', \vec{R}') \rangle / \langle I_\nu(\vec{r}, \vec{R}) \rangle \langle I_{\nu'}(\vec{r}', \vec{R}') \rangle , \quad (1)$$

where δI_ν is the deviation of the intensity from its ensemble average value, $\Delta r = |\vec{r} - \vec{r}'|$ and $\Delta R = |\vec{R} - \vec{R}'|$ are the displacements across the output and input surfaces, respectively, and $\langle \dots \rangle$ denotes the average over an ensemble of random realizations. The leading contribution to C obtained by factorizing the fields is [1, 2, 14, 22]:

$$C_1(\Delta r, \Delta R) = |\langle E_\nu(\vec{r}, \vec{R}) E_{\nu'}^*(\vec{r}', \vec{R}') \rangle|^2 / \langle I_\nu(\vec{r}, \vec{R}) \rangle \langle I_{\nu'}(\vec{r}', \vec{R}') \rangle . \quad (2)$$

The samples studied are random mixtures of 1.27-cm-diameter polystyrene spheres at a volume filling fraction of 0.52. They are contained inside a 100 cm long copper tube with a diameter of 7.5 cm capped with thin Plexiglas face plates. Field and intensity spectra are obtained in the frequency range 16.8 - 17.8 GHz with a step size of 625 kHz using a vector network analyzer. Measurements are taken in an ensemble of 690 random samples by rotating the tube to create new configurations of the spheres after each set of spectra are taken. Field spectra are obtained in each sample realization by translating an antenna detector along a line to each of 50 locations separated by 1.06 mm on the output surface for each of two fixed antenna sources at the incident surface, which are separated by $\Delta R = 3 \pm 0.1 \text{ cm} \equiv d$. Field spectra are also taken by translating the source along a line for each of two fixed antenna detectors at the output surface, separated by $\Delta r = d$. At the separation d , the short-range

term has largely decayed. The antennas are aligned perpendicular to the line of translation. Intensity spectra are obtained by squaring the field spectra.

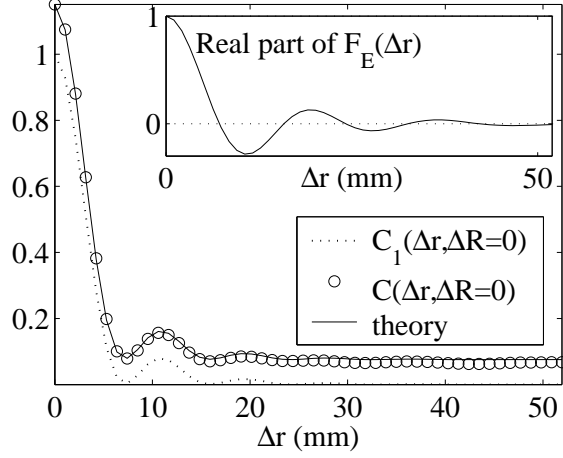


FIG. 1: Plots of $C(\Delta r, \Delta R=0)$ and $C_1(\Delta r, \Delta R=0)$, and theoretical fit to C .

The spatial variations of $C(\Delta r, 0)$ and $C_1(\Delta r, 0)$ are shown in Fig. 1. The C_1 contribution is directly obtained by squaring the field correlation function, shown in the inset of Fig. 1. Subtracting C_1 from the full intensity correlation function gives the difference $[C - C_1]$, shown in Fig. 2 for a single source ($\Delta R = 0$) and for two sources separated by $\Delta R = d$. This difference includes the terms beyond the field factorization approximation. Measurements

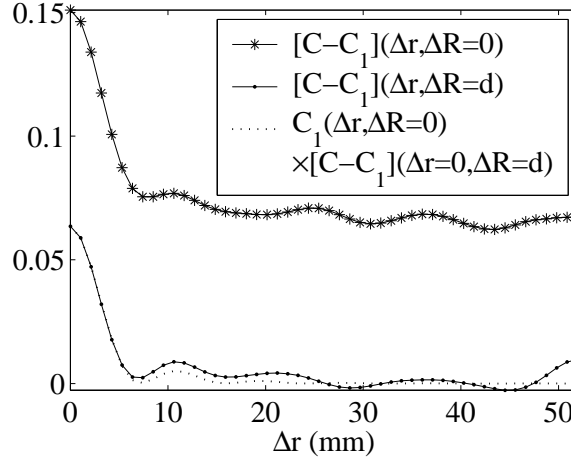


FIG. 2: plots of $[C - C_1](\Delta r)$ for $\Delta R = 0$ and 3 cm, and $C_1(\Delta r)$ at $\Delta R = 0$.

of $C(0, \Delta R)$ and $C_1(0, \Delta R)$, i.e. for a fixed detector and a scanning source, have also been performed. Within experimental error, $C(\Delta r, 0)$ and $C(0, \Delta R)$ were found to be identical

functions of their respective arguments. The same is true for C_1 . Similarly, we find that plots of $[C - C_1]$ versus ΔR with $\Delta r = 0$ and $\Delta r = d$ are nearly the same as those shown in Fig. 2. Thus ΔR and Δr can be interchanged as required by reciprocity.

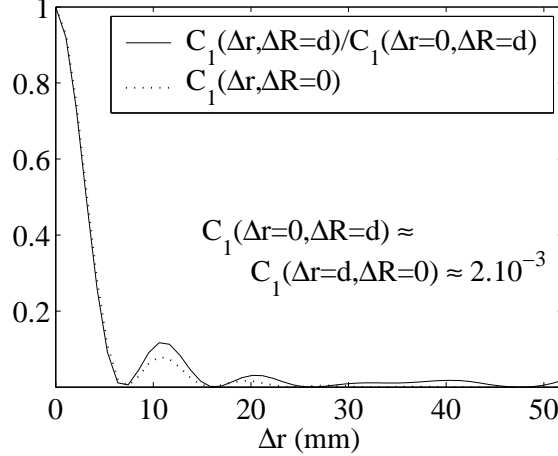


FIG. 3: Comparison of $C_1(\Delta r)$, normalized by its value at $\Delta r = 0$, for $\Delta R = 3$ cm and $C_1(\Delta r)$ at $\Delta R = 0$.

Measurements of $C_1(\Delta r, \Delta R)$ for $\Delta R = 0$ and $\Delta R = d$ are presented in Fig. 3. Within the noise level of 10^{-4} , the two functions have the same variation with Δr , $C_1(\Delta r, d) = 2 \times 10^{-3} C_1(\Delta r, 0)$. This numerical factor, $C_1(0, d)$, is equal to the value of $C_1(d, 0)$ within the uncertainty in d . This result, taken together with the aforementioned symmetry with respect to interchanging Δr and ΔR , suggests that C_1 can be written as the product of two identical functions, $C_1(\Delta r, \Delta R) = F(\Delta R)F(\Delta r)$.

We now examine $[C - C_1](\Delta r, \Delta R)$, which is dominated by C_2 in our sample. This function is seen in Fig. 2 to fall to nearly one half its value when either ΔR or Δr increase beyond δr when there is no displacement of the other variable. This shows that C_2 is given by the addition of two equal terms. The comparison of the short-range variation of $[C - C_1]$ with C_1 in Fig. 2 suggests that the additive form factors are identical to F , so that the dominant contribution to $C - C_1$ is proportional to $[F(\Delta R) + F(\Delta r)]$. This would imply that $C_2(\Delta r)$ approach a constant value for $\Delta r > \delta r$, whereas the measurement of $[C - C_1](\Delta r, d)$ is seen in Fig. 2 to fall slightly with increasing displacement. This could be the consequence of a slight departure from a quasi-1D geometry at the output face of the sample. There, the average intensity is slightly larger at the center than at the edges since the wave can spread beyond the cross section of the tube. Notwithstanding this effect,

our experimental results suggest that both C_1 and C_2 can be expressed in terms of a single form factor $F(x)$, where x stands for either Δr or ΔR . C_1 and C_2 contain, respectively, the product and the sum of two form factors. In Fig. 2, the correlation function $[C - C_1](\Delta r, d)$ is seen to lie above the dotted curve, which is proportional to C_1 . This suggests a constant contribution to C . For $\Delta r > 30$ mm, the correlation function becomes negative, but here the noise becomes larger than the signal because of the reduced number of pairs of points with increasing Δr . Such a long-range correlation for large values of ΔR may be part of C_3 .

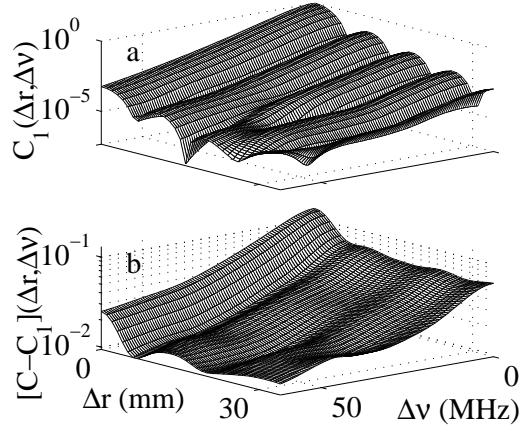


FIG. 4: Semilog representation of the spatial and frequency dependence of C_1 (a) and $[C - C_1]$ (b) for $\Delta R = 0$.

The structure of the joint spatial and frequency dependences of C_1 and C_2 , is obtained from measurements of the correlation functions $C_1(\Delta\nu, \Delta r)$ and $[C - C_1](\Delta\nu, \Delta r)$ for $\Delta R = 0$, shown in Figs. 4a and 4b, respectively. The semilog representations in Fig. 4 show that, within the limits set by the noise level, C_i have the same frequency dependence for any Δr , while C_i have the same spatial dependence for any $\Delta\nu$ for $i = 1, 2$. Thus their spatial and spectral variations for a single source are given by $C_i(\Delta\nu, \Delta r) = A_i(\Delta\nu)C_i(\Delta r)$. The noise level found in C_1 is low compared to that in C_2 because the field correlation function, F_E , is computed and then squared to obtain C_1 , giving a signal to noise ratio which is the square of that for the field correlation function. The form of the intensity correlation function suggested by experiment is borne out in diagrammatic calculations, which are briefly summarized below.

The three terms in C may be represented diagrammatically. The diagram corresponding to the C_1 term describes two non-interacting diffusons attached to pairs, GG^* , of averaged

Green's functions [7, 25]. This diagram factorizes into a product of two field functions:

$$\langle E_\nu(\vec{r}, \vec{R}) E_{\nu'}(\vec{r}', \vec{R}') \rangle = \int d^3 r_1 d^3 r_2 G_\nu(\vec{r}, \vec{r}_1) G_{\nu'}^*(\vec{r}', \vec{r}_1) T_{\nu\nu'}(\vec{r}_1, \vec{r}_2) G_\nu(\vec{r}_2, \vec{R}) G_{\nu'}^*(\vec{r}_2, \vec{R}') , \quad (3)$$

where $T_{\nu\nu'}(\vec{r}_1, \vec{r}_2)$ denotes the diffusion ladder and integration is performed over \vec{r}_1, \vec{r}_2 inside the tube. For the quasi one-dimensional geometry, the diffusion is independent of its transverse coordinates, whereas the Green's functions decay rapidly on a scale of the mean free path. Taking $\vec{R} = \vec{R}'$ and $\nu = \nu'$, we obtain

$$\langle E_\nu(\vec{r}, \vec{R}) E_\nu(\vec{r}', \vec{R}) \rangle = \left(\frac{4\pi}{\ell} \right) \int d^3 r_1 G_\nu(\vec{r}, \vec{r}_1) G_\nu^*(\vec{r}', \vec{r}_1) \langle I_\nu(\vec{r}_1, \vec{R}) \rangle \equiv F_E(\Delta r) , \quad (4)$$

where $I_\nu(\vec{r}, \vec{R})$ is the intensity at \vec{r} , normalized to its average value at the output face of the tube. Thus, $C_1(\Delta r, \Delta R) = F_E^2(\Delta r) F_E^2(\Delta R) \equiv F(\Delta R) F(\Delta r)$.

The diagrams corresponding to the C_2 and C_3 terms describe two incoming and two outgoing diffusons which interact in the bulk of the medium. In these diagrams, each pair GG^* of external Green's functions contributes a spatial form factor F_E as in Eq. (4). These give

$$\begin{aligned} C &= C_1 + C_2 + C_3 \\ &= A_1(\Delta\nu, \alpha) F(\Delta R) F(\Delta r) + \frac{2}{3g} A_2(\Delta\nu, \alpha) [F(\Delta R) + F(\Delta r)] \\ &\quad + \frac{2}{15g^2} A_3(\Delta\nu, \alpha) [1 + F(\Delta R) + F(\Delta r) + F(\Delta R) F(\Delta r)] , \end{aligned} \quad (5)$$

where g is the average conductance of the sample. The coefficients A_i ($i = 1, 2, 3$) depend on the absorption coefficient α and the frequency shift $\Delta\nu$. The structure of Eq. (5) is similar to that of the correlation in transmission, obtained in the multichannel formalism [3, 4, 7]. In the present case, however, all terms are described by a single spatial form factor. The field factorization term, $A_1(\Delta\nu = 0, \alpha)$ is unity and independent of absorption by definition, while $A_2(\Delta\nu = 0, \alpha)$ is given by [6, 23, 24]:

$$A_2(\Delta\nu = 0, \alpha) = \frac{3}{16\alpha} \left[\frac{\sinh 2\alpha - 2\alpha(2 - \cosh 2\alpha)}{\sinh^2 \alpha} \right] . \quad (6)$$

The coefficient $A_3(\alpha)$ depends weakly on α and its limiting values are $A_3(0) = 1, A_3(\infty) = 15/16$.

For our samples, $g \approx 7$ and $\alpha \approx 3$ [14]. From the measurement of $[C - C_1]$ at $\Delta r = 0$, $\frac{2}{3g} A_2 = 0.076$ with $A_2 = 0.87$. This is in agreement with Eq. (6) and calculated corrections

due to localization effects [6, 18, 23, 24, 25]. Using the measured $C_1(\Delta r)$ as the functional form $F(\Delta r)$, following Eq. (5) and neglecting C_3 , we obtain a good fit of the spatial structure of the intensity correlation function, as shown in Fig. 1.

These considerations have applications to present efforts to enhance the capacity of wireless communication by utilizing multiple antennas to detect the multiply scattered field [26, 27]. Antenna separation should be larger than δr and the number of statistically independent antennas equals the inverse of the degree of long-range intensity correlation, $3g/2$.

In conclusion, we have uncovered the connection between the field and intensity correlation functions in the spatial structure of the three contributions to C . In contrast to the case of angular correlation [3], intensity correlation can be expressed in terms of a single form factor obtained from the field correlation function. We have demonstrated the multiplicative character of C_1 and the additive character of C_2 . Calculations predict a mixed character for C_3 , which includes a multiplicative, an additive, and a constant term of equal amplitude. We observe the infinite-range component of C_3 in the residual correlation when both the source and detector are displaced by more than the correlation length. Determining the proper breakup of C into its components is of particular importance when considering simultaneous variations in space, time and frequency. Each term is a product of the corresponding C_1 , C_2 and C_3 correlation function in the appropriate variables.

We thank A.A. Chabanov for valuable discussions. Support from the National Science Foundation (DMR 9973959), Army Research Office (DAAD 190010362), the United States-Israel Binational Science Foundation (BSF) and the Groupement de Recherche PRIMA are gratefully acknowledged.

-
- [1] B. Shapiro, Phys. Rev. Lett. **57**, 2168 (1986).
 - [2] M. J. Stephen and G. Cwilich, Phys. Rev. Lett **59**, 285 (1987).
 - [3] S. Feng, C. Kane, P. A. Lee and A. D. Stone, Phys. Rev. Lett. **61**, 834 (1988).
 - [4] P. A. Mello, E. Akkermans and B. Shapiro, Phys. Rev. Lett. **61**, 459 (1988).
 - [5] A. Z. Genack, N. Garcia, and W. Polkosnik, Phys. Rev. Lett. **65**, 2129 (1990).
 - [6] E. Kogan and M. Kaveh, Phys. Rev. B **45**, 1049 (1992).
 - [7] M.C.W. Rossum and Th.M. Nieuwenhuizen, Rev. Mod. Phys. **71**, 313, 1999.

- [8] A point source embedded in the interior of a random medium exhibits an additional C_0 correlation, which can be larger than C_2 in some circumstances. B. Shapiro, Phys. Rev. Lett. **83**, 4733 (1999).
- [9] B. L. Altshuler, V. E. Kravtsov, and I. V. Lerner, in *Mesoscopic Phenomena in Solids*, edited by B. L. Altshuler, P. A. Lee, and R. A. Webb (Noth-Holland, Amsterdam, 1991).
- [10] R. A. Webb, S. Washburn, C. P. Umbach, and R. B. Laibowitz, Phys. Rev. Lett. **54**, 2696 (1985).
- [11] E. Abrahams, P. W. Anderson, D. C. Licciardello, and T. V. Ramakrishnan, Phys. Rev. Lett. **42**, 673 (1979).
- [12] I. Freund, M. Rosenbluh, and S. Feng, Phys. Rev. Lett. **61**, 2328 (1988).
- [13] J. H. Li and A. Z. Genack, Phys. Rev. E **49**, 4530 (1994).
- [14] P. Sebbah, R. Pnini and A. Z. Genack, Phys. Rev. E, **62**, 7348 (2000).
- [15] A. Z. Genack, Phys. Rev. Lett. **58**, 2043 (1987).
- [16] N. Garcia and A. Z. Genack, Phys. Rev. Lett. **63**, 1678 (1989).
- [17] M. P. van Albada, J. F. de Boer, and A. Lagendijk, Phys. Rev. Lett. **64**, 2787 (1990).
- [18] N. Garcia, A. Z. Genack, R. Pnini, and B. Shapiro, Phys. Lett. A **176**, 458 (1993).
- [19] G. Maret and P. E. Wolf, Z. Phys. B **65**, 409 (1987).
- [20] F. Scheffold, W. Härtl, G. Maret and E. Matijević, Phys. Rev. B **56**, 10942 (1997).
- [21] F. Scheffold and G. Maret, Phys. Rev. Lett. **81**, 5800 (1999).
- [22] I. Freund and D. Eliyahu, Phys. Rev. A **45**, 6133 (1992).
- [23] R. Pnini and B. Shapiro, Phys. Lett. A **157**, 265 (1991).
- [24] P. W. Brouwer, Phys. Rev. B **57**, 10526 (1998).
- [25] R. Pnini, in *Waves and Imaging through Complex Media*, ed. P. Sebbah (Kluwer Academic Publishers, the Netherlands) p.391-412.
- [26] A. L. Moustakas, H. U. Baranger, L. Balents, A. M. Sengupta, and S. H. Simon, Science **287**, 287 (2000).
- [27] S. H. Simon, A. L. Moustakas, M. Stoytchev, and H. Safar, Phys. Today (Sept. 2001) 34.